International Journal of Biological Macromolecules 283 (2024) 137019

Contents lists available at ScienceDirect

International Journal of Biological Macromolecules

journal homepage: www.elsevier.com/locate/ijbiomac

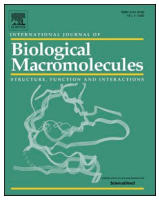

Effect of gum Arabic on antifungal photodynamic activity of curcumin against *Botrytis cinerea* spores

Maral Seididamyeh [a,*], Michael E. Netzel [a], Ram Mereddy [b], Jeffrey R. Harmer [c], Yasmina Sultanbawa [a]

[a] Centre for Nutrition and Food Sciences, Queensland Alliance for Agriculture and Food Innovation, The University of Queensland, Indooroopilly, QLD, 4068, Australia
[b] Department of Agriculture and Fisheries, Queensland Government, Coopers Plains, QLD 4108, Australia
[c] The Centre for Advanced Imaging, The University of Queensland, St Lucia, QLD 4072, Australia

ARTICLE INFO

Keywords:
Antifungal photodynamic treatment
Curcumin
Electron paramagnetic resonance spectroscopy

ABSTRACT

This study investigated the effect of gum Arabic on curcumin's phototoxicity against *Botrytis cinerea*, a significant cause of postharvest losses in horticultural produce. Curcumin-loaded nanoparticle suspensions and emulsions stabilized with gum Arabic were prepared and their absorbance, fluorescence emission, physicochemical properties, antimicrobial photodynamic activity (using response surface methodology (RSM)), and reactive oxygen species (ROS) generation (via electron paramagnetic resonance (EPR) spectroscopy) were evaluated. Fluorescence emission exhibited a blue shift (510–550 nm) in both formulations, with emulsions showing higher intensities due to a more hydrophobic environment. Gum Arabic concentration significantly influenced the physicochemical properties of both suspensions, with nanoparticle size decreasing from 572.80 nm to 202.80 nm as gum Arabic concentration increased from 0.5 % to 2.5 % (at 65 μM curcumin). Nanoparticle suspensions demonstrated higher antimicrobial efficacy, reducing *B. cinerea* spores by 0.39–3.40 $\log_{10}$(CFU.ml^{-1}), compared to 0.00–0.46 $\log_{10}$(CFU.ml^{-1}) in emulsions. The phototoxic effect was dependent on curcumin concentration and light irradiance, as demonstrated by RSM. EPR confirmed the generation of superoxide anion and hydroxyl radicals in both formulations, which indicated a Type I photodynamic mechanism, with nanoparticle suspensions having a sustained ROS generation. Overall, gum Arabic did not impair curcumin's antifungal photodynamic activity, making it as a promising stabiliser for curcumin-based treatments.

1. Introduction

The pathogenic fungal contamination of horticultural produce is a major cause of postharvest losses during storage and transport, which not only leads to severe economic losses but also poses a great threat to the food supply. One of the necrotrophic filamentous fungi, which infects a wide variety of fruits and vegetables is *Botrytis cinerea* that causes grey mold in postharvest stages. Various synthetic fungicides have been conventionally applied to control the *Botrytis* infection such as carbendazim, thiophanate-methyl, and pyrimethanil [1]. However, the chemical fungicides not only have shown potential harmful effects on environment and consumers, but also their excessive application has led to resistance development.

As a possible green alternative to the currently used chemical-based techniques in food industry, the antimicrobial photodynamic treatment has emerged with demonstrated cellular toxicity against a wide range of microorganisms. This treatment involves activating the applied photosensitizer by light of a specific wavelength and generating the cytotoxic reactive oxygen species such as singlet oxygen by transferring the energy from the excited photosensitizer to the cellular oxygen [2]. One of the main advantages of the photodynamic treatment is the multi-target damaging mechanism compared to the one distinct target mechanism of the synthetic fungicides [3], and therefore, there have not yet been any reports of the antimicrobial resistance of this technique.

Different natural photosensitizers are used for photodynamic treatment such as curcumin that is a hydrophobic polyphenol isolated from turmeric rhizome (*Curcuma longa*) and has shown promise as a cytotoxic photosensitizing molecule [4–6]. There are however several challenges for its application in food industry mainly due to its poor water solubility, which is about 3×10^{-8} M, and its poor chemical stability because

* Corresponding author.
E-mail addresses: s.maral@uq.edu.au (M. Seididamyeh), m.netzel@uq.edu.au (M.E. Netzel), ram.mereddy@daf.qld.gov.au (R. Mereddy), jeffrey.harmer@cai.uq.edu.au (J.R. Harmer), y.sultanbawa@uq.edu.au (Y. Sultanbawa).

https://doi.org/10.1016/j.ijbiomac.2024.137019
Received 16 June 2024; Received in revised form 25 October 2024; Accepted 27 October 2024
Available online 29 October 2024

of its high sensitivity to small changes in pH that leads to its hydrolytic degradation [7,8]. The poor water solubility of curcumin poses significant challenges in its application for antimicrobial photodynamic treatment, as it tends to aggregate in aqueous environment leading to reduction in light penetration and subsequently its availability and effectiveness. This has long been one of the main limitations for curcumin's application in photodynamic treatments. To this end, different encapsulating approaches have been investigated to overcome the limitations associated with curcumin such as liposomes [9], microgels [10], micelles [11], emulsions [12], and nanoparticles [13]. It has been shown that dispersibility and stability of curcumin in aqueous environments can be improved by incorporating them into colloidal structures such as the hydrophobic droplets within oil-in-water emulsions [7,14] as well as nanoparticle suspensions [15,16]. Natural biopolymers such as polysaccharides and proteins can be used to prepare curcumin-loaded nanoparticles, which have the ability to enhance the dispersibility and stability of poorly soluble compounds in aqueous environments. The electrostatic interactions by proteins are mainly responsible for their stabilizing behaviour. Therefore, protein-stabilized environments are prone to changes in environmental conditions such as pH, salt, and temperature, resulting in their instability [17]. On the other hand, steric interactions are the major mode of stabilization by polysaccharides such as gum Arabic (from *Acacia senegal*) and consequently are less affected by pH and salt [18,19]. It has also been reported that thermal treatment has less influence on polysaccharide-stabilized environments [19].

In this study, it is hypothesised incorporating curcumin in colloidal suspensions has no adverse impact on its phototoxicity and can in turn facilitate its applications in photo-decontamination treatments for food preservation. Therefore, curcumin loaded emulsion and nanoparticle suspension were prepared using gum Arabic as a commonly used edible biopolymer in food industry. Response surface methodology (RSM) was used to study the linear and interactive effects of influential parameters such as gum Arabic and curcumin concentrations as well as the illumination condition on the curcumin phototoxicity against *B. cinerea*.

Table 1
The I-optimal quadratic design and the actual values of the independent and dependent variables.

Run	Curcumin concentration (μM)	Gum arabic concentration (%)	Irradiance (mW. cm^{-2})	Light dose (J. cm^{-2})	Solvent	Log reduction (log_{10}(CFU. mL^{-1}))*	Cell Viability (%)*
1	35.75	2.50	31.75	42.79	Ethanol-MCT	0.46	43.29
2	6.50	0.50	31.75	19.05	Ethanol	0.65	49.70
3	35.75	1.50	44.35	19.05	Ethanol	1.75	27.36
4	35.75	2.50	38.57	66.53	Ethanol	1.06	19.84
5	65.00	0.50	44.35	66.53	Ethanol-MCT	0.16	44.15
6	65.00	2.50	44.35	19.05	Ethanol-MCT	0.00	51.12
7	35.75	1.50	38.57	42.79	Ethanol-MCT	0.00	44.91
8	65.00	1.50	38.57	42.79	Ethanol-MCT	0.00	41.87
9	35.75	1.50	31.75	42.79	Ethanol	1.77	13.97
10	35.75	1.50	31.75	42.79	Ethanol	2.44	5.03
11	65.00	2.50	31.75	19.05	Ethanol	1.32	22.73
12	65.00	2.50	44.35	42.79	Ethanol	2.63	15.29
13	6.50	2.50	44.35	42.79	Ethanol-MCT	0.00	49.81
14	35.75	1.50	38.57	42.79	Ethanol-MCT	0.00	41.96
15	65.00	2.50	44.35	42.79	Ethanol	3.34	9.14
16	6.50	0.50	44.35	19.05	Ethanol-MCT	0.12	33.10
17	6.50	0.50	31.75	66.53	Ethanol-MCT	0.07	45.73
18	6.50	2.50	31.75	66.53	Ethanol	0.39	67.58
19	35.75	1.50	44.35	19.05	Ethanol	3.09	5.66
20	35.75	0.50	38.57	66.53	Ethanol	1.53	11.69
21	65.00	0.50	38.57	19.05	Ethanol	0.75	26.01
22	6.50	1.50	38.57	42.79	Ethanol	0.58	49.80
23	35.75	1.50	44.35	66.53	Ethanol-MCT	0.00	51.05
24	65.00	2.50	31.75	66.53	Ethanol-MCT	0.35	74.15
25	65.00	0.50	31.75	66.53	Ethanol	0.57	68.28
26	6.50	2.50	38.57	19.05	Ethanol	0.39	49.92
27	6.50	1.50	31.75	19.05	Ethanol-MCT	0.14	39.97
28	6.50	0.50	44.35	66.53	Ethanol	0.75	62.35
29	35.75	1.50	38.57	42.79	Ethanol-MCT	0.00	42.22
30	65.00	1.50	38.57	66.53	Ethanol	1.52	9.05
31	35.75	1.50	31.75	66.53	Ethanol-MCT	0.10	59.53
32	65.00	0.50	31.75	19.05	Ethanol-MCT	0.00	41.40
33	35.75	0.50	38.57	42.79	Ethanol-MCT	0.26	36.91
34	65.00	2.50	44.35	66.53	Ethanol-MCT	0.00	61.19

* Results are the average of six replications.

Furthermore, spin-trapping electron paramagnetic resonance was used to determine the reactive oxygen species generation during photosensitization process.

2. Materials and methods

2.1. Design of experiments

An I-optimal quadratic design including 6 replicate centre points and 6 lack-of-fit points was generated by a randomised RSM (Design Expert, v.11.1.2.0, Stat-Ease, Minneapolis, MN, USA) to study the effects of five factors including curcumin concentration, gum Arabic concentration, irradiance, light dose, and solvent, and their interactions on curcumin phototoxicity against *B. cinerea* spores (Table 1). The least-squares method was applied for assessing the factors in polynomial approximation and response surface analysis was performed via the fitted surface. In the case that the fitted surface is a sufficient approximation of the real response function, then those analyses would be nearly equal to actual system analysis. Significant models for antimicrobial photodynamic activity in terms of log reduction and viability of *B. cinerea* spores were generated by variance analysis using Design Expert software and the significant effects as well as interactive factors of those responses were determined.

2.2. Preparation of nanoparticle suspension and emulsion

Curcumin (from *C. longa*, ≥ 65 %, Sigma-Aldrich, St Louis, MO, USA) stock solutions (4000 μM; *w/v*) were prepared in ethanol (99.8 %, Fisher Chemical, Loughborough, UK) and in the mixture (1:1, *v*/v) of ethanol and MCT oil (derived from coconut oil (C8, C10), 100 %, Melróse, Mt. Waverley, VIC, Australia), and were kept at −20 °C for one week. Gum Arabic (Acrōs Organics, UK) stock solutions (5, 3, and 1 %; w/v) were prepared in ultrapure water (Milli-Q, Millipore, Burlington, MA, USA) under magnetic stirring for 1 h. The prepared solutions were kept overnight at 4 °C for complete hydration and dissolution. To prepare the emulsion and nanoparticle suspension, the curcumin dissolved in (respectively) ethanol-MCT and ethanol was slowly added to the gum Arabic solution with constant stirring using a magnetic stirrer. The volume ratio of curcumin to gum Arabic solution in the final working system was 1:20. It was then mixed for 2 min using high speed homogenizer (24,000 rpm, IKA T25D Ultraturrax, Staufen, Germany), followed by 4 min sonication (30 % Amplitude (A), continuous; SFX550 Sonifier, Branson, Mexico) in an ice bath. The prepared emulsions and nanoparticles were kept at 4 °C for 5 days.

2.3. Characterization of nanoparticle and emulsion

The visible absorption and fluorescence emission spectra for curcumin nanoparticle suspensions and emulsions were obtained using a spectrophotometer (Varioskan LUX 3020–80,884, Thermo Scientific, Singapore). The absorbance spectra were recorded within 300–700 nm (1-nm steps) and the fluorescence emission spectra within 450–750 nm (430 nm as excitation wavelength, 1-nm slit width). The polydispersity index, mean particle diameter, and zeta potential of curcumin nanoparticle suspensions and emulsions were measured at room temperature using dynamic light scattering and electrophoresis (Zetasizer Ultra, Malvern Instruments, Worcestershire, UK). Samples were diluted using ultrapure water to avoid multiple scattering effects [20]. The colour values were measured by a chromameter (CR-400, Konica Minolta, Tokyo, Japan) using a black sheet as the background. The instrument was calibrated with a standard white tile. A given volume of sample was placed into a transparent disposable petri dish. The measurements were expressed as L* (lightness (+) and darkness (−)), a* (redness (+) and greenness (−)), and b* (yellowness (+) and blueness (−)) [20]. All measurements were performed on freshly made suspensions in at least triplicate and at room temperature.

2.4. Spore suspension preparation

The spore suspension was harvested from the 2-week-old culture of *B. cinerea* [21], which was isolated from the commercial strawberry cultivar 'Red Rhapsody' grown in Queensland, Australia [22]. Potato dextrose agar (CM0139, Oxoid, Basingstoke, Hampshire, UK) was used as culture media. The suspension was counted using a Haemocytometer and kept at 4 °C and used within a week.

2.5. Antimicrobial photodynamic activity

To determine the antimicrobial activity, the spore suspension (10^5 CFU.mL^{-1}) was prepared in both sterile ultrapure water and potato dextrose broth (PDB; Sigma-Aldrich). Briefly, 50 μL of the curcumin suspensions were incubated with 50 μL of spore suspension, followed by illumination under LED light (420 nm, 200 W, 100–240 V; COB LED Light Fixture, HYG05–4, China) for the given time (Table 1). The light irradiance of the treatment was determined by measuring the photosynthetic photon flux density of LEDs at 10 different positions at a 10-cm distance from the light source [21]. The dark control samples were incubated for 10 min in darkness at room temperature in the presence of different curcumin suspensions. For a negative control representing 0 μM of curcumin, sterile ultrapure water or PDB was added. To determine the effect of photodynamic treatment on *B. cinerea* growth, 30 μL of the homogenized treated sample was spread-plated on *Botrytis* selective media (prepared according to [23]), and incubated at 25 °C for 4 days. The results were reported as $\log_{10}$ (CFU.mL^{-1}) reduction. Tetrazolium dye (MTT) assay was also carried out to further evaluate the survival rate of the spores [24], where 10 μL of aqueous MTT solution (5 mg.mL^{-1}; EMD Millipore Group, Darmstadt, Germany) was added to the samples. After incubation at 25 °C for 2 h, the media was removed, 200 μL dimethyl sulfoxide (Sigma-Aldrich) was added, mixed, and incubated overnight at 25 °C to enhance the dissolution. Then, the fungal plug was removed and absorbance at 570 nm was measured (Infinite M200, Tecan GmbH, Grödig, Austria) and the results were reported as percentage of viability [21].

2.6. Determination of reactive oxygen species

Spin-trapping electron paramagnetic resonance (EPR) spectroscopy was used to detect, identify, and measure the photo-generated reactive oxygen species using 5,5-dimethyl-pyrroline N-oxide (DMPO; 80 mM; >97 %, Chem-Supply, Gillman, SA, Australia) and alpha-phenyl N-tertiary-butyl nitrone (PBN; 80 mM; ≥98 %, Sigma-Aldrich) as spin traps [21]. Equal aliquots of curcumin suspensions and spin trap solutions were mixed and directly illuminated (420 nm, 15 min, 43.59 and 62.71 mW.cm^{-2}) in an X-band continuous wave (CW) EPR cavity. Experimental parameters used for EPR operating in X-band (Bruker, Rheinstetten, Germany) include 100 kHz modulation frequency, 19.82 mW microwave power, ca. 9.87 GHz microwave frequency, 3518 G central field, 110 G sweep width, 41.94 s sweep time, and 3 G modulation amplitude. The EPR spectra of control samples (without curcumin) under illumination/darkness and curcumin suspensions under darkness were also recorded. The spectral identification of the spin adducts were confirmed by simulating the spectra with known hyperfine coupling constants [25–29] and comparing them with the experimentally observed one using MATLAB software (R2020b, MathWorks Inc., Natick, MA, USA). TEMPO (4-hydroxy-2,2,6,6-tetramethyl-1-piperidimyloxy; 98 %; Fujifilm Wako, Japan) radical was used to quantify the generated spin adducts. All the EPR measurements were conducted at room temperature and in triplicate.

3. Results and discussion

3.1. Absorbance and fluorescence

The absorption and fluorescence emission spectra of curcumin nanoparticle suspensions and emulsions are depicted in Fig. S1. The prominent absorbance band was shown to be around 420 nm, which is characteristic of curcumin's π-π* transitions, which aligns with previous reports for curcumin in various environments [21]. This was less broad than in aqueous ethanolic environments without gum Arabic [21], where the lack of clear maxima suggests curcumin aggregation due to poor solubility. The inclusion of gum Arabic, even in lower concentrations, minimizes aggregation by stabilizing curcumin through encapsulation and surface interactions [20], which allows for clearer spectral features. Furthermore, an increase in curcumin concentration led to an increase in the absorbance intensity for all nanoparticle suspensions (Fig. S1.a, b, c) with gum Arabic concentration having less influence. However, the curcumin emulsions exhibited much stronger absorbance intensities that exceeded the detection range of the spectrophotometer and therefore are not reported here. This is likely due to the higher turbidity of emulsions and the scattering effects caused by the dispersed oil droplets, and therefore light scattering and absorption are amplified at the incident wavelength range [30,31]. Moreover, MCT oil's ability to prevent curcumin nucleation in the environment increases its solubilization, and consequently enhances absorbance intensity.

Fluorescence emission spectra provided additional insights into curcumin's behaviour in different environments. The observed blue shift in fluorescence emission from 560 to 570 nm in aqueous ethanolic environments [21] to 510–550 nm in nanoparticle suspensions suggests that gum Arabic influences curcumin's excited-state dynamics by altering its local environment (Fig. S1.d, e, f). Higher concentrations of curcumin and gum Arabic correlate with increased fluorescence intensity, likely due to reduced aggregation and enhanced solubility of curcumin. At lower gum Arabic concentrations, the reduced emission intensity is consistent with aggregation, where insufficient biopolymer stabilizes fewer curcumin molecules (Fig. S1.d). In emulsions, the blue shift of the emission peak to 47–481 nm, alongside stronger fluorescence, indicates a more hydrophobic environment induced by MCT oil that promotes a more pronounced fluorescent response (Fig. S1.g, h, i). The relative decline in fluorescence intensity at 2.5 % gum Arabic concentration suggests that the excess gum Arabic may entrap curcumin more efficiently and therefore reduces its availability for fluorescence (Fig. S1.i). Overall, the enhanced fluorescence emission in emulsions compared to nanoparticle suspensions highlights the impact of medium and curcumin concentration on its spectral properties. Fluorescence emission intensity is closely linked to curcumin's photodynamic activity and its ability to generate ROS. In fact, fluorescence emission intensity reflects how much of the absorbed light energy is dissipated as fluorescence, which competes with the process of intersystem crossing to the triplet state that undergoes interaction with molecular oxygen to generate ROS [32,33]. If more energy is emitted as fluorescence, as was observed for emulsions, less is available to promote intersystem crossing and therefore reduces the amount of ROS generated. However, in some cases, higher fluorescence emission can indicate better curcumin dispersal in the environment and less aggregation, which improves the overall efficiency of light absorption and energy transfer. This can thus lead to a more efficient generation of ROS despite the competition between fluorescence and intersystem crossing. Hence, optimizing curcumin's formulation to balance fluorescence emission with ROS generation is essential for maximizing its photodynamic antimicrobial effect.

3.2. Physicochemical characterization

The physicochemical properties of curcumin-loaded nanoparticles and emulsions are presented in Table 2. Results showed that mean particle size, polydispersity index, and zeta potential were strongly influenced by the concentration of curcumin and gum Arabic. At lower curcumin concentrations (6.5 μM), an increase in gum Arabic concentration leads to larger particle sizes and more negative zeta potentials. However, an increase in gum Arabic at higher curcumin concentrations (35.75 and 65 μM) resulted in smaller particle sizes and lower polydispersity indices, which indicates more uniform particles. The size reduction can be attributed to the enhanced electrostatic repulsion that prevents aggregation and stabilizes smaller particles [34]. The particle sizes of these suspensions are almost in the range of 100–200 nm and therefore are considered as nanoparticles [35]. In general, nanoparticle is strictly defined as particles with <100 nm particle size, while in practice is referred to particles within the range of 1–1000 nm [36].

In curcumin emulsions, increasing gum Arabic concentration led to a decrease in mean droplet size, regardless of curcumin concentration (Table 2). This is due to the presence of more gum Arabic molecules in the environment to form a protective layer around the surface of curcumin-contained oil droplets generated by homogenization [20]. The relatively large protein-polysaccharide structure of gum Arabic effectively attaches to the oil-water interface by the amphiphilic polypeptide chain while the large hydrophilic polysaccharide chain is into the

Table 2
The parameters of curcumin nanoparticle suspensions and curcumin emulsions using different concentrations of curcumin and gum Arabic.

Gum arabic (%)	Curcumin (μM)	Mean particle size (nm)	Polydispersity Index	Zeta potential (mV)	L*	a*	b*
Curcumin nanoparticle suspension							
0.50	**6.50**	123.30 ± 11.29	0.39 ± 0.01	−19.77 ± 2.52	34.69 ± 0.09	−0.66 ± 0.09	4.12 ± 0.51
0.50	**35.75**	262.37 ± 32.29	0.62 ± 0.12	−12.51 ± 1.98	34.07 ± 0.59	−4.56 ± 0.01	21.90 ± 0.82
0.50	**65.00**	572.80 ± 28.70	0.82 ± 0.07	−27.58 ± 1.07	35.05 ± 0.41	−3.97 ± 0.30	28.80 ± 0.70
1.50	**6.50**	150.30 ± 24.47	0.47 ± 0.05	−23.47 ± 5.95	36.55 ± 0.73	−1.25 ± 0.14	4.80 ± 0.48
1.50	**35.75**	180.30 ± 23.71	0.57 ± 0.23	−33.09 ± 1.51	35.60 ± 0.47	−5.76 ± 0.11	25.77 ± 1.43
1.50	**65.00**	200.77 ± 23.45	0.46 ± 0.05	−32.95 ± 3.93	34.12 ± 0.71	−3.12 ± 0.18	30.96 ± 0.86
2.50	**6.50**	218.70 ± 28.96	0.48 ± 0.05	−34.58 ± 3.83	36.18 ± 0.66	−1.88 ± 0.18	6.71 ± 0.56
2.50	**35.75**	198.87 ± 3.78	0.48 ± 0.00	−36.51 ± 2.94	35.22 ± 1.61	−6.00 ± 0.16	25.95 ± 1.81
2.50	**65.00**	202.80 ± 12.77	0.55 ± 0.02	−39.74 ± 4.46	34.97 ± 1.64	−4.74 ± 0.43	30.58 ± 0.39
Curcumin emulsion							
0.50	**6.50**	912.40 ± 44.95	0.16 ± 0.03	−43.69 ± 1.78	72.82 ± 1.04	−5.77 ± 0.33	7.24 ± 0.77
0.50	**35.75**	905.90 ± 92.51	0.31 ± 0.13	−43.70 ± 0.73	73.75 ± 1.06	−13.85 ± 0.32	26.95 ± 1.20
0.50	**65.00**	598.60 ± 21.52	0.22 ± 0.08	−44.01 ± 1.36	76.45 ± 0.92	−16.15 ± 0.19	36.44 ± 1.30
1.50	**6.50**	1081.47 ± 184.40	0.22 ± 0.01	−42.98 ± 0.22	74.76 ± 1.36	−6.16 ± 0.43	8.62 ± 1.12
1.50	**35.75**	782.60 ± 61.37	0.14 ± 0.05	−42.51 ± 1.55	76.61 ± 0.20	−14.56 ± 0.05	30.51 ± 0.28
1.50	**65.00**	556.07 ± 15.35	0.17 ± 0.03	−42.54 ± 0.36	78.26 ± 0.73	−16.49 ± 0.05	38.79 ± 1.04
2.50	**6.50**	501.73 ± 29.18	0.26 ± 0.09	−42.58 ± 0.76	77.80 ± 0.66	−4.54 ± 0.17	4.65 ± 0.57
2.50	**35.75**	553.25 ± 65.52	0.25 ± 0.05	−43.23 ± 1.09	77.89 ± 1.22	−13.93 ± 0.27	28.60 ± 1.56
2.50	**65.00**	540.63 ± 65.39	0.21 ± 0.07	−43.22 ± 0.72	78.50 ± 0.37	−16.67 ± 0.03	39.68 ± 0.60

Results are means (± standard error) of at least three replications.

surrounding aqueous environment [37]. Therefore, this unique structure leads to its slow adsorption rate and high surface load [38,39], which means higher amount of gum Arabic is needed per unit surface area of oil droplets in emulsions to be covered. Thus, droplet coalescence in emulsion at lower gum Arabic concentration can occur and induce higher droplet sizes.

A larger particle size of 572.80 nm was observed at 65 μM curcumin and 0.5 % gum Arabic (Table 2), which is likely due to the insufficient concentration of gum Arabic to stabilize the higher curcumin content. The increased particle size can be attributed to curcumin's hydrophobic nature, which promotes self-association and aggregation in aqueous environments. As gum Arabic concentration increased to 1.5 % and 2.5 %, more consistent particle/droplet sizes were achieved, which suggests that the higher biopolymer content improved stabilization. This stabilization likely occurred due to the enhanced emulsifying action of gum Arabic, together with the homogenizer's efficiency in breaking down and dispensing particles or oil droplets more effectively [20]. Moreover, as droplet size reduces through homogenization, the resistance to further size reduction increases due to rising Laplace pressure. This effect is particularly evident in emulsions, as described by the Laplace pressure equation ($\Delta P = \frac{4\gamma}{D}$), where the pressure difference across the droplet interface (ΔP) increases as the oil-water interfacial tension (γ) rises and droplet diameter (D) decreases [40]. In this study, a high-speed homogenizer operating at 24,000 rpm followed by 4 min of sonication at 30 % amplitude was used to disperse the curcumin phase into the gum Arabic solution. These results indicate the need for further investigation into the influence of homogenization parameters such as speed, sonication power, and time on the mean particle/droplet size. The dependency of particle/droplet size on biopolymer concentration has also been reported in previous studies [20,41,42], which highlights the importance of optimization in achieving desired particle/droplet sizes.

The zeta potential results also suggest that gum Arabic plays a role in enhancing the stability of curcumin-loaded systems by providing sufficient negative surface charge, which ranged from −12.51 to −39.74 mV for nanoparticle suspensions and from −42.51 to −44.01 mV for emulsions (Table 2). The surface charge of the nanoparticles was influenced by the concentration of gum Arabic, while the zeta potential of the emulsions remained unaffected by changes in curcumin or gum Arabic concentrations. The observed negative charge is attributed to the deprotonation of carboxyl groups (–COO^-), which are fully ionized at neutral pH ($pK_a = 3.5$) [43] and are present on the hydrophilic polysaccharide chains of gum Arabic. This in turn stabilizes the suspensions and emulsions by preventing particle aggregation through repulsive forces between negatively charged particles [44]. Higher zeta potential magnitudes correspond to better stability, particularly in nanoparticle suspensions, where aggregation can significantly impact performance and availability of curcumin. This stabilizing effect is essential for maintaining the uniform dispersion of curcumin in colloidal systems, thus improving its functional properties.

Additionally, the effect of different concentrations of curcumin and gum Arabic on the colour properties of nanoparticle suspensions and emulsions was determined by measuring the tristimulus colour coordinates (L*, a* and b*). While the concentrations of curcumin and gum Arabic did not affect the lightness (L*) of the samples, emulsions exhibited higher lightness values than the nanoparticles, which may be attributed to better dispersion of curcumin in the emulsion environment. Moreover, results showed that increasing curcumin concentration resulted in more intense green (negative a*) and yellow (positive b*) values, particularly in emulsions. All suspensions and emulsions showed negative a* values, indicating a slight green hue, where emulsions exhibited more pronounces green tones with a* values ranging from −4.54 to −16.67, compared to nanoparticle suspensions (−0.66 to −6.00). Positive b* values across all samples indicated that the yellow coloration is primarily driven by curcumin content. Overall, these findings determine the importance of biopolymer concentration in optimizing the physicochemical properties of curcumin-loaded delivery systems for enhanced stability and functionality in various applications.

3.3. Antimicrobial photodynamic activity

The comparison of curcumin's phototoxicity in two colloidal suspensions, namely nanoparticle and emulsion, was performed using RSM with an I-optimal design. RSM was used to examine the interaction effects between multiple factors including curcumin and gum Arabic concentrations, irradiance, light dose, and solvent on the photoinactivation efficiency of curcumin against *B. cinerea* spores. The antimicrobial photodynamic activity of curcumin was assessed by log reduction and spore viability (referred to as cell viability in graphs) as response variables in the study. These responses were selected to assess how the dispersion of curcumin in gum Arabic might affect its phototoxicity, with illumination parameters incorporated as independent variables. The design matrix and corresponding results are detailed in Table 1, which demonstrate the effect of these factors on curcumin's antimicrobial performance.

Model fitting and statistical significance of the independent variables were determined through multiple regression analysis. Insignificant polynomial terms ($p > 0.05$) were excluded from the initial model, which resulted in a refined model that retained only significant terms to develop a significant model ($p < 0.05$). The adequacy of the quadratic models was further validated using ANOVA, and the results are given in Table 3 and Figs. S2-S3. A second-order polynomial equation was employed to mathematically describe the experimental data derived from the I-optimal design. The relationship between the independent variables and the response variables, namely log reduction (R_1) and spore viability (R_2), was exhibited in the empirical reduced quadratic models (Table 3), both of which were highly significant ($p < 0.0001$) that confirm the robustness of the models in predicting curcumin's photodynamic activity.

The log reduction in *B. cinerea* spores varied from 0.00 to 3.34 $\log_{10}$ ($CFU.mL^{-1}$) and cell viability varied from 5.03 % to 74.15 % (Table 1). Factors such as curcumin concentration, gum Arabic concentration, and illumination conditions significantly influenced the antimicrobial photodynamic activity of the colloidal suspensions. Figs. 1 and S4 illustrate the effects of these factors and their interactions on curcumin's efficacy in photo-decontaminating *B. cinerea* spores. Solvent played a key role in determining the phototoxicity of curcumin within colloidal environments (Table 3, Fig. 1), which is consistent with findings in non-colloidal environments [21]. Therefore, nanoparticles formed with ethanol-dissolved curcumin exhibited significantly enhanced antimicrobial activity compared to emulsions ($p < 0.05$), which was evidenced by a higher log reduction and lower cell viability (Table 1). This is likely due to the increased availability of curcumin to microbial cells [45], which facilitates higher cellular uptake and enhances the antimicrobial photodynamic effect. In contrast, emulsions showed lower photoinactivation efficiency, which can possibly be attributed to curcumin entrapment within the hydrophobic cores of MCT oil micelles [46], which restricts its interaction with spore cell walls and reduces overall phototoxicity (Fig. 1.b,d and S4.b,d). This observation is consistent with prior findings, suggesting that hydrophobic cores limit the availability of curcumin to generate ROS effectively.

Furthermore, curcumin concentration was as a critical factor significantly affecting the efficacy of photodynamic treatment ($p < 0.05$). This effect is attributed to the amount of curcumin available in proximity to spore cells, which can be photoexcited to generate reactive oxygen species. The results showed enhanced antimicrobial activity as curcumin concentration increased from 6.5 to 39 μM, beyond which no further improvement was observed. This optimal concentration not only improves antimicrobial efficacy, but also prevents curcumin aggregation in the environment, which can hinder photoinactivation efficiency. Gum Arabic, while playing a key role in stabilizing colloidal suspensions, showed no significant effect on phototoxicity determined by log

Table 3
Analysis of variance of the predicted models for *Botrytis cinerea* log reduction and cell viability.

Source	Sum of squares	Df	mean square	F-value	*p*-value	
Reduced quadratic model (square root transform (0.5)) - log reduction						
Model	4.30	9	0.4778	22.48	< 0.0001	Significant
A-Curcumin Concentration	0.2285	1	0.2285	10.75	0.0032	
C-Irradiance	0.0922	1	0.0922	4.34	0.0480	
D-Light Dose	0.0085	1	0.0085	0.4009	0.5326	
E-Solvent	3.16	1	3.16	148.91	< 0.0001	
AE	0.0819	1	0.0819	3.85	0.0614	
CE	0.2117	1	0.2117	9.96	0.0043	
A^2	0.1891	1	0.1891	8.90	0.0065	
C^2	0.3714	1	0.3714	17.48	0.0003	
D^2	0.1585	1	0.1585	7.46	0.0117	
Residual	0.5100	24	0.0213			
Lack of Fit	0.3926	19	0.0207	0.8799	0.6246	Not significant
Pure Error	0.1174	5	0.0235			
Cor Total	4.81	33				
Fit Statistics						
Std. Dev.	**Mean**	**C.V. (%)**	**R^2**	**Adjusted R^2**	**Predicted R^2**	**Adeq precision**
0.15	1.06	13.72	0.89	0.85	0.78	14.82
Predicted Model	$\sqrt{R_1 + 0.5} = 1.10 + 0.11\ A + 0.06C - 0.02D - 0.31E - 0.06AE - 0.10\ CE - 0.17A^2 + 0.24C^2 - 0.16D^2$					
Reduced quadratic model - spore viability						
Model	8161.23	7	1165.89	7.42	< 0.0001	significant
A-Curcumin Concentration	869.29	1	869.29	5.53	0.0266	
B-Gum Arabic Concentration	30.41	1	30.41	0.1934	0.6637	
D-Light Dose	838.99	1	838.99	5.34	0.0291	
E-Solvent	2086.76	1	2086.76	13.27	0.0012	
AE	1278.49	1	1278.49	8.13	0.0084	
BE	657.50	1	657.50	4.18	0.0511	
A^2	1797.06	1	1797.06	11.43	0.0023	
Residual	4087.76	26	157.22			
Lack of Fit	3788.10	21	180.39	3.01	0.1123	not significant
Pure Error	299.66	5	59.93			
Cor Total	12,248.98	33				
Fit Statistics						
Std. Dev.	**Mean**	**C.V. (%)**	**R^2**	**Adjusted R^2**	**Predicted R^2**	**Adeq precision**
12.54	38.70	32.40	0.67	0.58	0.39	9.19
Predicted Model	$R_2 = 29.45 - 6.63\ A + 1.22B + 6.31\ D + 7.93E + 8.01AE + 5.70BE + 15.15A^2$					

reduction or spore viability (Fig. 1.a, S4.a). However, interaction plots revealed that optimizing both curcumin and gum Arabic concentrations can further enhance antimicrobial activity in both nanoparticles and emulsions (Fig. S4.b). This improvement is likely due to gum Arabic's role in enhancing curcumin dispersibility in aqueous environments, which leads to reduced curcumin aggregation and increases its availability for ROS generation. These findings suggest that gum Arabic primarily stabilizes the colloidal system rather than directly influencing curcumin's phototoxicity.

Illumination parameters, including light irradiance and light dose, also play a significant role in determining the antimicrobial efficiency of curcumin-based photodynamic treatment (Table 3). These parameters determine the intensity of light exposure and total energy delivered to the treatment area, respectively. Our findings indicated that light dose significantly influenced curcumin's phototoxicity in colloidal environments ($p < 0.05$). A quadratic relationship between irradiance, light dose, and the log reduction of *B. cinerea* spores suggested an optimal light dose of approximately 42.8 J.cm^{-2} (Table 3), beyond which no additional antimicrobial effect was observed. In addition, increasing irradiance >38 mW.cm^{-2} resulted in a notable increase in log reduction (Fig. 1). The non-linear behaviour of light parameters is likely due to the balance between curcumin excitation and ROS generation, and therefore excessive light doses potentially lead to curcumin degradation or photobleaching giving rise to a reduced efficacy. Synergistic effects between curcumin concentration and irradiance further enhanced photodynamic efficacy (Fig. S4) that demonstrates the complex dynamics of photodynamic treatment and highlights the importance of optimizing light conditions for effective antimicrobial activity. The findings demonstrated the phototoxic potential of curcumin nanoparticle suspensions, which supports the potential use of gum Arabic as a carrier for the hydrophobic curcumin. The interplay and non-linear response observed in the RSM plots underscores the complexity of these systems and emphasizes the need for optimizing multiple factors to develop effective curcumin-based antimicrobial treatments. Additionally, the lack of antimicrobial activity in dark and negative control samples (data not shown) confirmed the dependency of curcumin's activity on light activation, which indicates the photodynamic nature of its antimicrobial effect on *B. cinerea* spores.

Several studies have demonstrated promising results in enhancing curcumin's solubility through the use of biopolymers, without compromising its photosensitizing efficacy. For instance, Preis and colleagues achieved significant antimicrobial reductions of 6.1 and 1.6 $\log_{10}$ (CFU.g^{-1}) in *Staphylococcus saprophyticus* subsp. *bovis* and *Escherichia coli* DH5α, respectively, by utilizing redispersed spray-dried curcumin nanoparticles in mannitol matrix [47]. Similarly, Li and co-workers (2020) reported a 5 $\log_{10}$ (CFU.g^{-1}) reduction in *S. aureus* after 10 min of illumination using curcumin-loaded chitosan (25 μg.mL^{-1} curcumin) [48]. In our study, this approach was extended by investigating the interaction of multiple factors affecting the efficacy of antimicrobial photodynamic treatment against *B. cinerea*. By optimizing the variables, the optimal conditions for maximizing log reduction and minimizing spore viability were determined. The optimized parameters included 49.05 μM ethanolic curcumin, 2.50 % gum Arabic, irradiance of 44.35 mW.cm^{-2}, and a light dose of 30.21 J.cm^{-2}. Subsequent experiments using these conditions resulted in a 3.52 $\log_{10}$ (CFU.g^{-1}) reduction and 7.05 % spore viability, that closely aligned with the predicted outcomes (2.85 $\log_{10}$ (CFU.g^{-1}) and 10.18 % spore viability), thus validating the effectiveness of our model in optimizing curcumin-based antimicrobial photodynamic treatment.

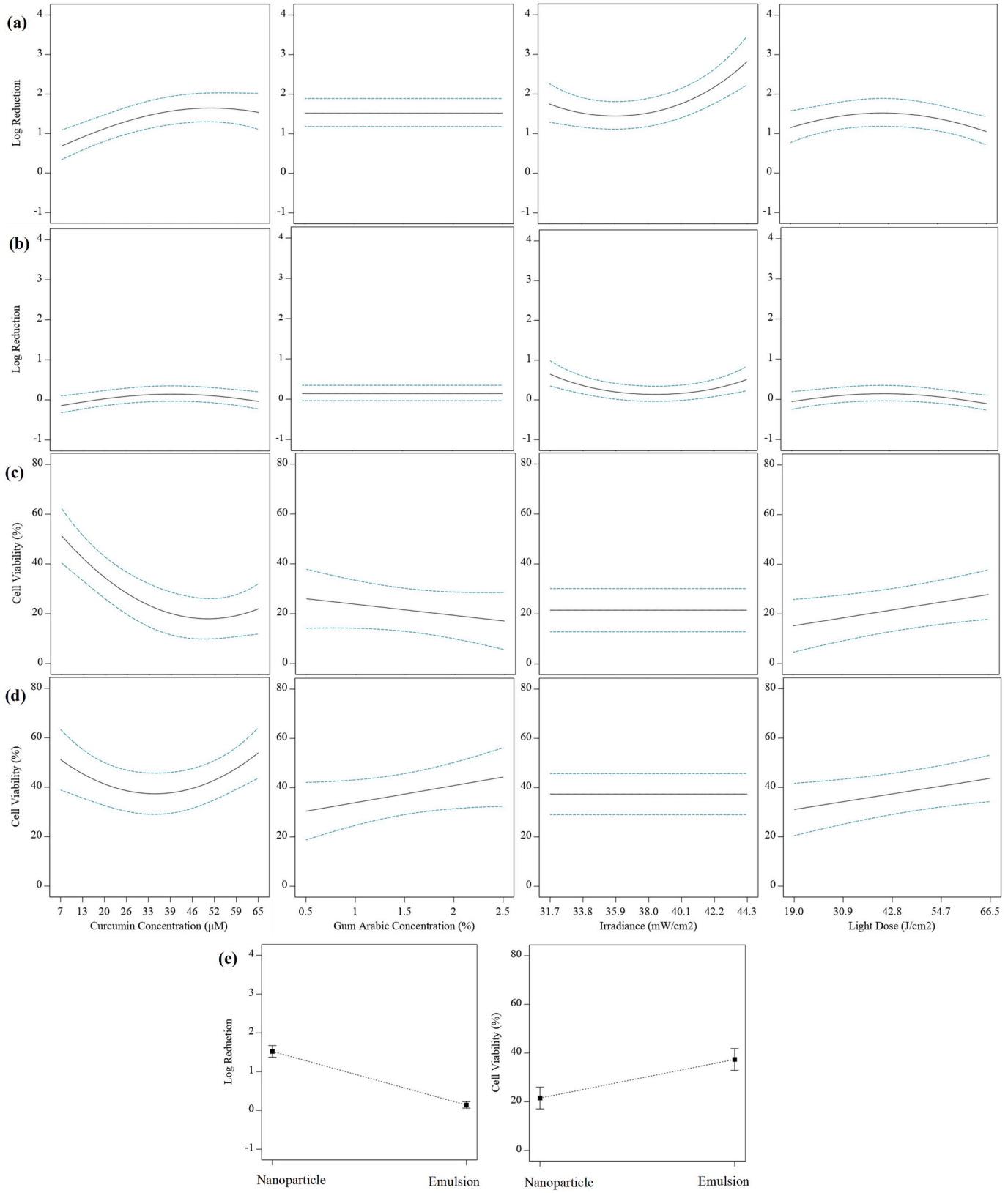

Fig. 1. Effects of independent variables on *Botrytis cinerea* log reduction (log_{10} (CFU.ml^{-1})) in nanoparticle suspension (a) and emulsion (b) and its cell viability (%) in nanoparticle suspension (c) and emulsion (d), and solvent (d) at constant condition of 35.75 μM curcumin, 1.5 % gum Arabic, 38.05 mW.cm^{-2} irradiance, 42.79 J. cm^{-2} light dose.

3.4. Photoinduced generation of reactive oxygen species

EPR spin trapping spectroscopy was employed to confirm the generation of reactive oxygen species (ROS) in curcumin nanoparticle suspensions and emulsions, using DMPO and PBN as spin traps. This technique provides valuable insights into the photodynamic behaviour of curcumin. As illustrated in Figs. 2 and S5-S7, both formulations effectively generated superoxide anion ($O_2^{\bullet-}$) and hydroxyl ($OH^{\bullet}$) radicals upon exposure to visible light at 420 nm. The EPR spectra from both suspensions showed similar complex patterns (Fig. 2.a-h), and the simulation of spectra indicated the simultaneous formation of four distinct DMPO adducts derived from $O_2^{\bullet-}$, $OH^{\bullet}$, hydroxyethyl ($OC_2H_5^{\bullet}$), and unpaired DMPO$^{\bullet}$ radicals [25,26,28] during the photodynamic activation of curcumin. The detection of additional radicals such as hydroxyethyl radical adducts suggests the involvement of secondary radical-mediated oxidation processes, where curcumin's excited triplet state may interact with surrounding molecules that results in the formation of alkyl or oxygen radicals. These radicals may react with cellular components and contribute to further oxidation and cellular damage, and therefore enhancing the antimicrobial photodynamic effect.

Additionally, PBN spin trapping in nanoparticle suspensions revealed PBN-OH$^{\bullet}$ adducts in the simulated spectra [28], which provided further confirmation of the photo-generation of hydroxyl radicals. As shown in Fig. 2.i-l, PBN forms a more stable adduct with hydroxyl radicals, which allows for detection of ROS production over a longer period. These findings are consistent with previous studies on curcumin solutions [21], which demonstrates that gum Arabic does not interfere with curcumin's ability to generate ROS through Type I photodynamic mechanism. Curcumin transfers electrons or hydrogen atoms to molecular oxygen, and forms superoxide anions and hydroxyl radicals. The formation of multiple radical adducts supports this direct electron transfer pathway. These results align with findings by Hariharan et al. [49], who observed superoxide anion and hydroxyl radicals photogeneration in curcumin-loaded ZnO nanocomposites [49]. Moreover, no EPR spectra signals were detected without curcumin or light (data not shown), which confirms that ROS generation is strictly dependent on light activation.

The evolution of radical adducts over a 15-min illumination period is illustrated in Figs. 3–4 and S8-S9, showing a similar pattern to the previous findings [21]. The concentration of radical adducts, which serve as a proxy for ROS levels, was determined by comparing the double integration of EPR signals with a known concentration of the stable radical TEMPO. It was found that ROS levels were significantly influenced by curcumin and gum Arabic concentrations, light irradiance, and illumination time. Both formulations exhibited increased ROS generation with higher curcumin and gum Arabic concentrations. At 62.71 mW.cm^{-2}, nanoparticle suspensions containing 65 μM curcumin showed a rapid rise in ROS-adduct concentrations, reaching peak levels before declining – from 1.71 μM in 0.5 % gum Arabic to 3.78 μM in 2.5 % gum Arabic (Fig. 3.b, d, f). This peak likely results from higher energy provided by intense illumination, which not only accelerates curcumin excitation and ROS production but also affects the ROS lifetime. Additionally, higher energy levels may lead to the rapid degradation of curcumin by triggering reactive interactions within the surrounding environment. In contrast, lower irradiance (43.59 mW.cm^{-2}) produced a more gradual and sustained ROS generation profile (Fig. S8.a, c, e), which indicates a slower, more controlled generation of ROS over time.

A direct relationship between curcumin concentration and ROS generation demonstrates the dose-dependent nature of the

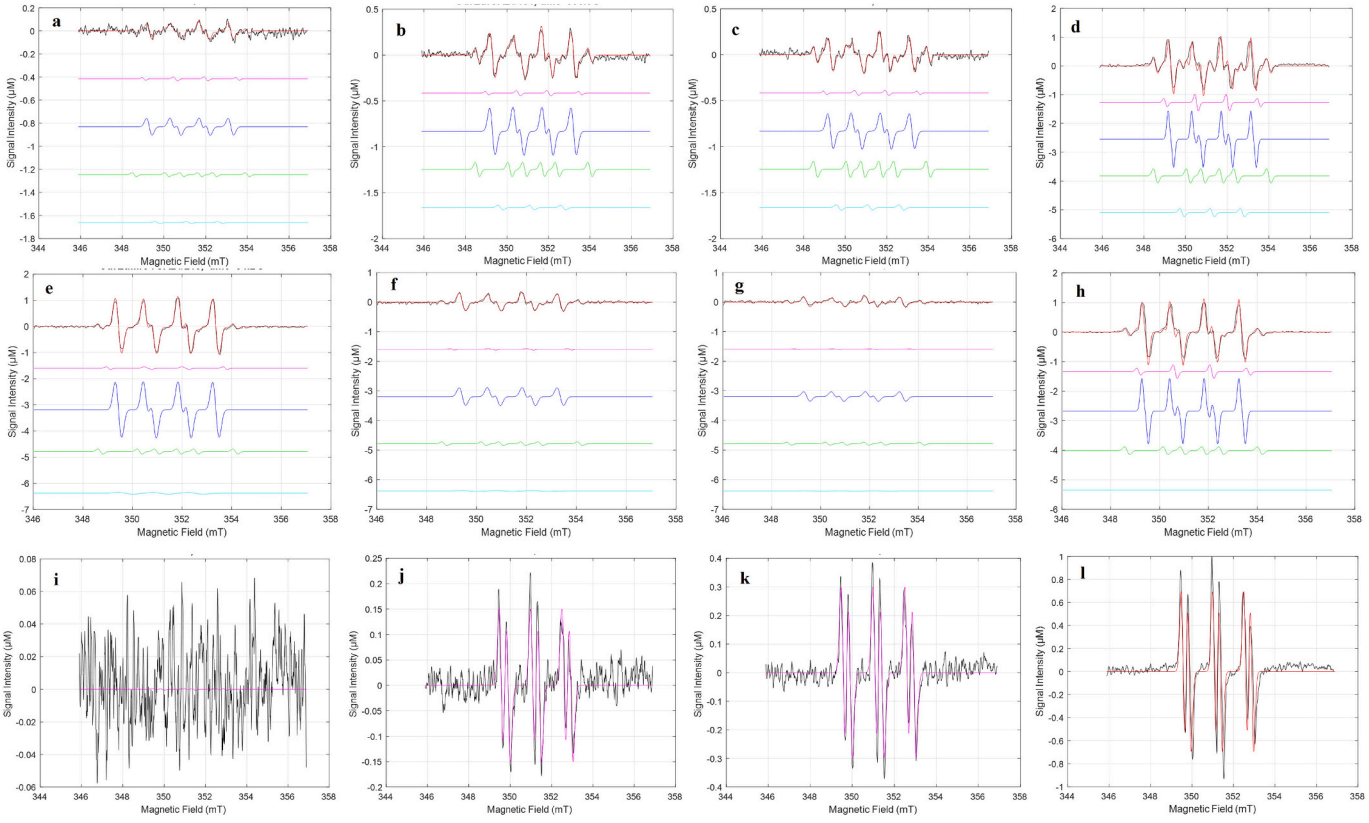

Fig. 2. Experimental (black line) and simulated EPR spectra (red line) for curcumin nanoparticle suspension and emulsion (65 μM curcumin, 1.5 % GA, 15 min illumination at 62.71 mW.cm^{-2}). DMPO-ROS adducts including DMPO-hydroxyl adduct (magenta), DMPO-superoxide anion adduct (blue), DMPO-hydroxyethyl adduct (green) and DMPO radical (cyan); using nanoparticle suspension after 44.2 s (a), 515 s (b), 909.3 s (c), and the average of 15 min (d) illumination; using emulsion after 44.2 s (e), 515 s (f), 909.3 s (g), and the average of 15 min (h) illumination. PBN-ROS adducts including PBN-hydroxyl adduct (magenta) after 44.2 s (i), 515 s (j), 909.3 s (k), and the average of 15 min (l) illumination.

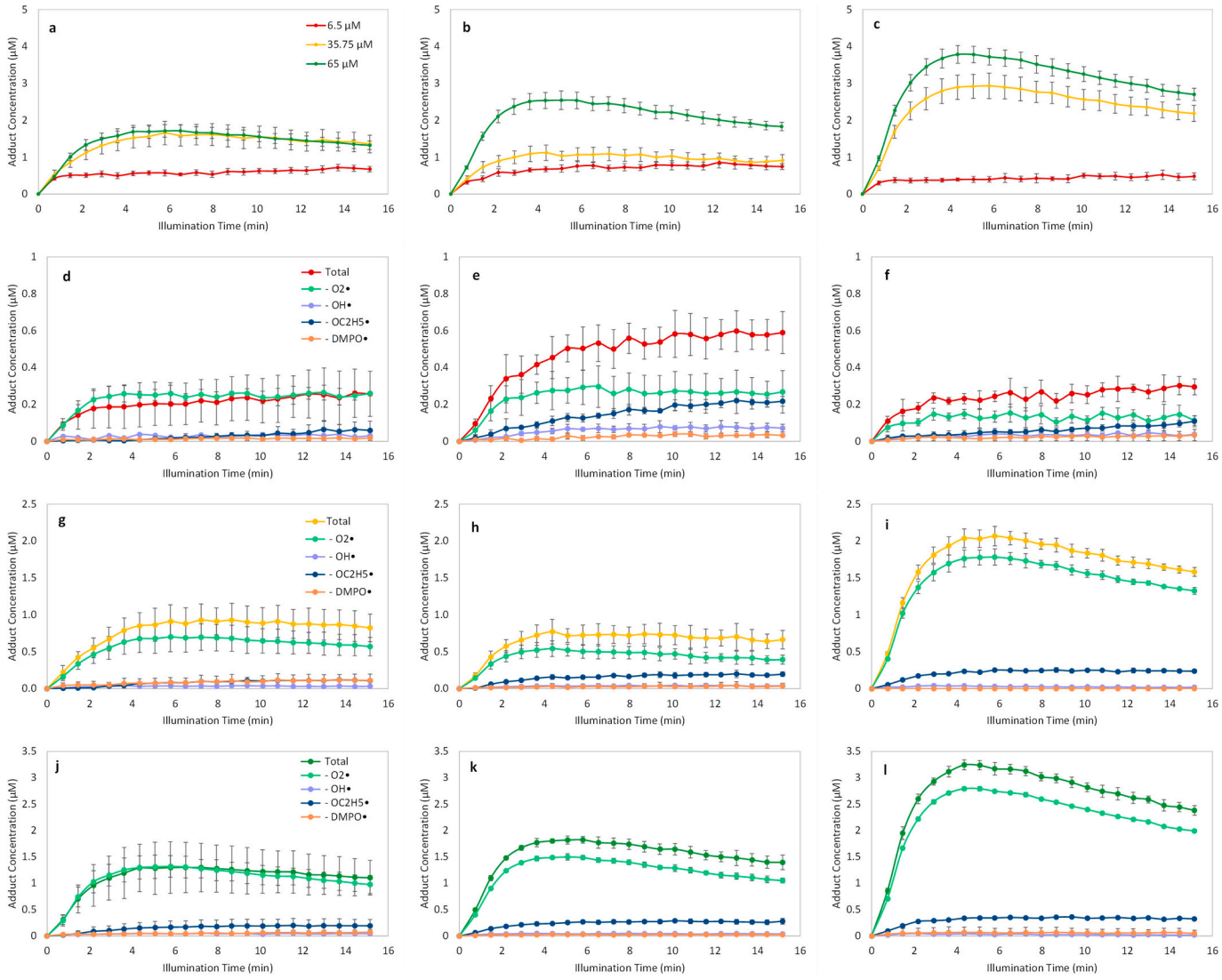

Fig. 3. Evolution of total (experimental) adduct and simulated and fitted radical adduct concentration (μM) over 15 min illumination of nanoparticle suspensions (6.5, 35.75 and 65 μM curcumin) at 62.71 mW.cm^{-2} using DMPO as spin trap: total radical adduct formation, in (a) 0.5 % GA, (b) 1.5 % GA, (c) 2.5 % GA, and simulated radical adducts in (d) 0.5 % GA, 6.5 μM curcumin, (e) 1.5 % GA, 6.5 μM curcumin, (f) 2.5 % GA, 6.5 μM curcumin, (g) 0.5 % GA, 35.75 μM curcumin, (h) 1.5 % GA, 35.75 μM curcumin, (i) 2.5 % GA, 35.75 μM curcumin, (j) 0.5 % GA, 65 μM curcumin, (k) 1.5 % GA, 65 μM curcumin, (l) 2.5 % GA, 65 μM curcumin. The results are the mean of at least three replicates. The error bar indicates the standard error of at least three replicates.

photodynamic process, which is consistent with other studies [21,50,51]. Higher curcumin levels enhance photosensitization-induced oxidation on nanoparticle surfaces [52], leading to the release of entrapped curcumin. On the other hand, gum Arabic serves as a stabilizing agent and improves curcumin dispersion in the aqueous environment, which reduces aggregation [44] and enhances the surface area of the photosensitizer exposed to light. This results in a more uniform light absorption and efficient interaction with molecular oxygen, and in turn promotes ROS generation and forming more radical adducts. Without gum Arabic, curcumin tends to form aggregates, which can reduce its overall surface area exposed to light. These aggregates are less sufficient at absorbing light and transferring energy to molecular oxygen, resulting in reduced ROS production as shown in previous study [21].

However, increasing gum Arabic to 2.5 % in emulsions with 6.5 and 35.75 μM curcumin reduced ROS generation (Fig. 4.f, i), which is consistent with fluorescence emission observations (Fig. S1.i). While gum Arabic enhances the physical stability of curcumin in emulsions, higher concentrations encapsulate curcumin and limit the availability of free curcumin molecules at the surface of emulsion droplets and the surrounding environment. Therefore, the ROS generation is reduced as the light-triggered release of curcumin relies on these free molecules for the occurrence of photosensitization-induced oxidation [52]. This suggests the need to optimise gum Arabic concentration for enhancing the stability and activity of curcumin without compromising its release.

Nanoparticle suspensions demonstrated a sustained increase in ROS generation during the illumination period, which is indicative of prolonged photodynamic activity. Emulsions, by contrast, showed an initial ROS burst, followed by rapid degradation or quenching of ROS. This could be due to the instability of DMPO-superoxide anion adducts (DMPO-OOH; lifetime<1 min [53]) and quenching effect of emulsion components, such as MCT oil, which can act as radical scavengers [54] and reduce the overall effectiveness of the photodynamic process. This suggests that curcumin is more readily available for light activation in nanoparticle form, with minimal quenching or degradation of the radicals. This pattern, also seen in gum Arabic-free environments [21], may explain higher in vitro phototoxicity of nanoparticle suspensions against *B. cinerea* spores compared to emulsions.

PBN spin trapping and illumination at 62.71 mW.cm^{-2} confirmed increased hydroxyl radical generation in nanoparticle suspensions

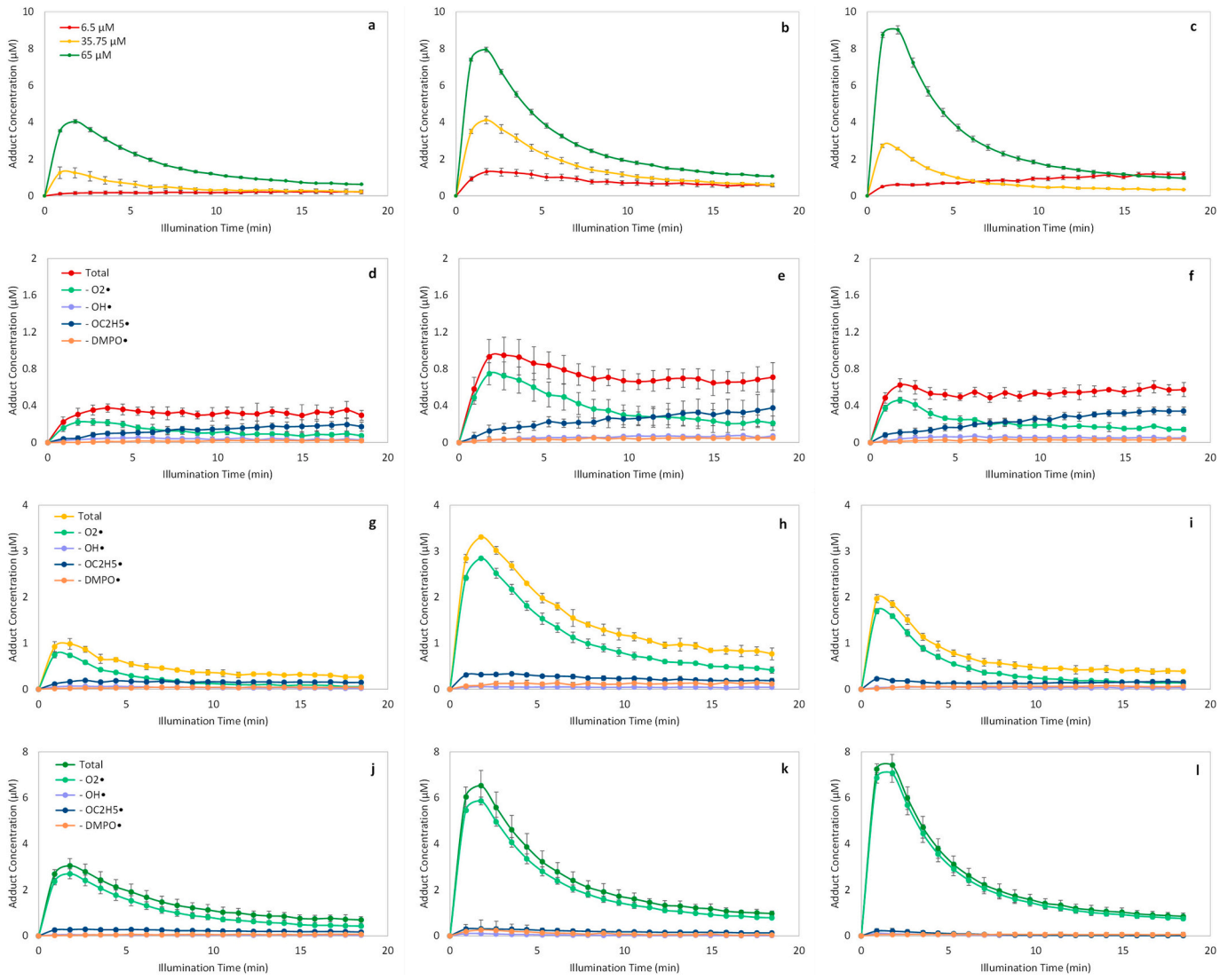

Fig. 4. Evolution of total (experimental) adduct and simulated and fitted radical adduct concentration (µM) over 15 min illumination of emulsion (6.5, 35.75 and 65 µM curcumin) at 62.71 mW.cm^{-2} using DMPO as spin trap: total radical adduct formation in (a) 0.5 % GA, (b) 1.5 % GA, (c) 2.5 % GA, and simulated radical adducts in (d) 0.5 % GA, 6.5 µM curcumin, (e) 1.5 % GA, 6.5 µM curcumin, (f) 2.5 % GA, 6.5 µM curcumin, (g) 0.5 % GA, 35.75 µM curcumin, (h) 1.5 % GA, 35.75 µM curcumin, (i) 2.5 % GA, 35.75 µM curcumin, (j) 0.5 % GA, 65 µM curcumin, (k) 1.5 % GA, 65 µM curcumin, (l) 2.5 % GA, 65 µM curcumin. The results are the mean of at least three replicates. The error bar indicates the standard error of at least three replicates.

(Fig. S9). However, when curcumin concentration exceeded 35.75 µM, ROS generation plateaued that indicated a saturation point beyond which additional curcumin does not enhance photodynamic activity. Overall, both nanoparticle suspensions and emulsions are effective in generating ROS, however, parameters such as gum Arabic concentration, and light conditions need optimization to maximise curcumin's photodynamic activity. These findings contribute to the broader understanding of formulation effects on the performance of curcumin as photosensitizer in antimicrobial photodynamic treatment.

4. Conclusion

This study investigated the impact of various parameters on antimicrobial photodynamic activity of curcumin-loaded nanoparticle suspensions and emulsions against *B. cinerea* spores using RSM and EPR spin trapping spectroscopy. The use of an I-optimal design in RSM was effective in exploring the interactive effects of various factors on curcumin's phototoxicity, which highlighted the dependency on curcumin concentration and irradiance. EPR spectroscopy confirmed the generation of ROS by both formulations, particularly superoxide anion and hydroxyl radicals under visible light activation. The EPR study suggested that curcumin retains its photodynamic behaviour regardless of its colloidal form and supports a multi-faceted ROS generation mechanism in both formulations driven by Type I photodynamic mechanism and secondary radical-mediated oxidation. Nanoparticle suspensions exhibited a higher photoinactivation of spores compared to emulsions, which was attributed to improved curcumin dispersibility in aqueous environment and sustained ROS generation during illumination, as indicated by EPR studies. EPR studies also showed a direct relation between ROS generation and concentrations of curcumin and gum Arabic as well as light irradiance. Although further research should focus on further optimizing formulation parameters and explore long-term stability and effectiveness of gum Arabic-curcumin systems in practical applications. Overall, this study showed the potential of gum Arabic as an effective stabiliser for enhancing curcumin's photodynamic activity and suggests curcumin nanoparticle suspension as a more stable and effective alternative to oil-based emulsions for photo-decontamination applications. These findings offer valuable insights for tailoring these formulations for broad range of applications by varying curcumin and gum Arabic concentrations and optimizing illumination condition to

modulate ROS generation.

Funding declaration

This work was supported by Horticulture Innovation Australia Limited (HN15001 Naturally Nutritious project) and the Australian Research Council (ARC) Industrial Transformation Training Centre (ITTC) for Uniquely Australian Foods (Grant number: IC180100045).

CRediT authorship contribution statement

Maral Seididamyeh: Writing – original draft, Methodology, Investigation, Formal analysis, Conceptualization. **Michael E. Netzel:** Writing – review & editing, Supervision. **Ram Mereddy:** Writing – review & editing, Supervision. **Jeffrey R. Harmer:** Writing – review & editing, Methodology. **Yasmina Sultanbawa:** Writing – review & editing, Supervision, Resources, Funding acquisition.

Declaration of competing interest

The authors declare the following financial interests/personal relationships which may be considered as potential competing interests: Yasmina Sultanbawa reports financial support was provided by University of Queensland. Yasmina Sultanbawa reports financial support was provided by Horticulture Innovation Australia Ltd.

Acknowledgement

Maral Seididamyeh acknowledges the support from the Australian Government via the Research Training Program Scholarship for her doctorate studies at the University of Queensland (Brisbane, QLD, Australia). The authors thank Margaret Currie and Andrew Cusack (Department of Agriculture and Fisheries, QLD, Australia) for their technical support.

Appendix A. Supplementary data

X-band CW EPR spectrometer set-up (Figure), absorbance and fluorescence emission spectra of curcumin solutions (Figure), additional information on data analysis (Table, Figure), surface graphs of curcumin in MCT contained environments (Figure), EPR spectra (Figure). https://doi.org/10.1016/j.ijbiomac.2024.137019.

Data availability

The datasets generated during and/or analysed during the current study are available from the corresponding author on reasonable request.

References

[1] W.M. Jurick, O. Macarisin, V.L. Gaskins, E. Park, J. Yu, W. Janisiewicz, K.A. Peter, Characterization of postharvest fungicide-resistant *Botrytis cinerea* isolates from commercially stored apple fruit, Phytopathology 107 (3) (2017) 362–368.
[2] T.D. Le, P. Phasupan, K. Visaruthaphong, P. Chouwatat, V.T. Thu, L.T. Nguyen, Development of an antimicrobial photodynamic poly (3-hydroxybutyrate-co-3-hydroxyvalerate) packaging film for food preservation, Food Packag. Shelf Life 30 (2021) 100749.
[3] T. Maisch, R.-M. Szeimies, G. Jori, C. Abels, Antibacterial photodynamic therapy in dermatology, Photochem. Photobiol. Sci. 3 (10) (2004) 907–917.
[4] T.Q. Correa, K.C. Blanco, E.B. Garcia, S.M.L. Perez, D.J. Chianfrone, V.S. Morais, V. S. Bagnato, Effects of ultraviolet light and curcumin-mediated photodynamic inactivation on microbiological food safety: a study in meat and fruit, Photodiagn. Photodyn. Ther. 30 (2020) 101678.
[5] C. Gong, Y. Li, R. Gao, F. Xiao, X. Zhou, H. Wang, H. Xu, R. Wang, P. Huang, Y. Zhao, Preservation of sturgeon using a photodynamic non-thermal disinfection technology mediated by curcumin, Food Biosci. 36 (2020) 100594.
[6] B.B. Saraiva, B.M. Rodrigues, R.C. da Silva Junior, M.R. da Silva Scapim, C.A. C. Lancheros, C.V. Nakamura, W. Caetano, P.C. de Souza Pereira, E.H.W. de Santana, M.S. dos Santos Pozza, Photodynamic inactivation of *Pseudomonas fluorescens* in Minas Frescal cheese using curcumin as a photosensitizer, LWT-Food Science and Technology 151 (2021) 112143.
[7] M. Kharat, Z. Du, G. Zhang, D.J. McClements, Physical and chemical stability of curcumin in aqueous solutions and emulsions: impact of pH, temperature, and molecular environment, J. Agric. Food Chem. 65 (8) (2017) 1525–1532.
[8] M. Tomren, M. Masson, T. Loftsson, H.H. Tønnesen, Studies on curcumin and curcuminoids: XXXI. Symmetric and asymmetric curcuminoids: stability, activity and complexation with cyclodextrin, Int. J. Pharm. 338 (1–2) (2007) 27–34.
[9] S. Peng, L. Zou, W. Liu, C. Liu, D.J. McClements, Fabrication and characterization of curcumin-loaded liposomes formed from sunflower lecithin: impact of composition and environmental stress, J. Agric. Food Chem. 66 (46) (2018) 12421–12430.
[10] Z. Zhang, R. Zhang, L. Zou, L. Chen, Y. Ahmed, W. Al Bishri, K. Balamash, D. J. McClements, Encapsulation of curcumin in polysaccharide-based hydrogel beads: impact of bead type on lipid digestion and curcumin bioaccessibility, Food Hydrocoll. 58 (2016) 160–170.
[11] F. Ye, D. Lei, S. Wang, G. Zhao, Polymeric micelles of octenylsuccinated corn dextrin as vehicles to solubilize curcumin, LWT–Food Sci. Technol. 75 (2017) 187–194.
[12] K. Ahmed, Y. Li, D.J. McClements, H. Xiao, Nanoemulsion-and emulsion-based delivery systems for curcumin: encapsulation and release properties, Food Chem. 132 (2) (2012) 799–807.
[13] H. Xie, C. Xiang, Y. Li, L. Wang, Y. Zhang, Z. Song, X. Ma, X. Lu, Q. Lei, W. Fang, Fabrication of ovalbumin/κ-carrageenan complex nanoparticles as a novel carrier for curcumin delivery, Food Hydrocoll. 89 (2019) 111–121.
[14] L. Zou, B. Zheng, R. Zhang, Z. Zhang, W. Liu, C. Liu, G. Zhang, H. Xiao, D. J. McClements, Influence of lipid phase composition of excipient emulsions on curcumin solubility, stability, and bioaccessibility, Food Biophys. 11 (3) (2016) 213–225.
[15] S. Peng, L. Zhou, Q. Cai, L. Zou, C. Liu, W. Liu, D.J. McClements, Utilization of biopolymers to stabilize curcumin nanoparticles prepared by the pH-shift method: Caseinate, whey protein, soy protein and gum Arabic, Food Hydrocoll. 107 (2020) 105963.
[16] A. Ubeyitogullari, O.N. Ciftci, A novel and green nanoparticle formation approach to forming low-crystallinity curcumin nanoparticles to improve curcumin's bioaccessibility, Sci. Rep. 9 (1) (2019) 1–11.
[17] R. Charoen, A. Jangchud, K. Jangchud, T. Harnsilawat, O. Naivikul, D. J. McClements, Influence of biopolymer emulsifier type on formation and stability of rice bran oil-in-water emulsions: whey protein, gum Arabic, and modified starch, J. Food Sci. 76 (1) (2011) E165–E172.
[18] Y. Liu, Z. Hou, J. Yang, Y. Gao, Effects of antioxidants on the stability of β-carotene in O/W emulsions stabilized by gum Arabic, J. Food Sci. Technol. 52 (6) (2015) 3300–3311.
[19] Y. Wu, N. Eskin, W. Cui, B. Pokharel, Emulsifying properties of water soluble yellow mustard mucilage: a comparative study with gum Arabic and citrus pectin, Food Hydrocoll. 47 (2015) 191–196.
[20] M. Kharat, G. Zhang, D.J. McClements, Stability of curcumin in oil-in-water emulsions: impact of emulsifier type and concentration on chemical degradation, Food Res. Int. 111 (2018) 178–186.
[21] M. Seididamyeh, M.E. Netzel, R. Mereddy, J.R. Harmer, Y. Sultanbawa, Photodynamic inactivation of *Botrytis cinerea* spores by curcumin—effect of treatment factors and characterization of photo-generated reactive oxygen species, Food Bioprocess Technol. (2023) 1–16.
[22] M. Seidi Damyeh, C.W. Fernando, A.D.T. Phan, H.T. Hong, R. Mereddy, M. E. Netzel, M. Chaliha, Y. Sultanbawa, Post-harvest fungal occurrence on commercial strawberry cultivars grown in Australia: impact of phytochemical composition, J. Food Meas. Charact. 15 (2021) 3811–3822.
[23] S. Edwards, B. Seddon, Selective media for the specific isolation and enumeration of *Botrytis cinerea* conidia, Lett. Appl. Microbiol. 32 (2) (2001) 63–66.
[24] N. Shamali, A. Preuß, I. Saltsman, A. Mahammed, Z. Gross, G. Däschlein, B. Röder, In vitro photodynamic inactivation (PDI) of pathogenic germs inducing onychomycosis, Photodiagn. Photodyn. Ther. 24 (2018) 358–365.
[25] D.G. Della Rocca, H.F. Victoria, C.D. Moura-Nickel, G. Scaratti, K. Krambrock, A. De Noni, V.J. Vilar, H.J. Jose, R.F. Moreira, Peroxidation and photo-peroxidation of pantoprazole in aqueous solution using silver molybdate as catalyst, Chemosphere 262 (2021) 127671.
[26] N.J. Dodd, A.N. Jha, Photoexcitation of aqueous suspensions of titanium dioxide nanoparticles: an electron spin resonance spin trapping study of potentially oxidative reactions, Photochem. Photobiol. 87 (3) (2011) 632–640.
[27] R.V. Lloyd, P.M. Hanna, R.P. Mason, The origin of the hydroxyl radical oxygen in the Fenton reaction, Free Radic. Biol. Med. 22 (5) (1997) 885–888.
[28] C.S. Monteiro, D.C. Ferreira, G.A. Sáfar, R.N. Gontijo, C. Fantini, D.C. Martins, Y. M. Idemori, M.V. Pinheiro, K. Krambrock, Unravelling the mechanisms of reactive oxygen species formation in nanohybrid systems of porphyrins and enriched (6, 5) single-walled carbon nanotubes for photosensitization, Phys. Chem. Chem. Phys. 18 (30) (2016) 20459–20465.
[29] C. Mottley, H.D. Connor, R.P. Mason, [17O] oxygen hyperfine structure for the hydroxyl and superoxide radical adducts of the spin traps DMPO, PBN and 4-POBN, Biochem. Biophys. Res. Commun. 141 (2) (1986) 622–628.
[30] M.T. Celis, L.H. Garcia-Rubio, Spectroscopy as a tool for characterization of monomer emulsions, J. Dispers. Sci. Technol. 28 (2) (2007) 271–278.
[31] B. Glasse, C. Assenhaimer, R. Guardani, U. Fritsching, Turbidimetry for the stability evaluation of emulsions used in machining industry, Can. J. Chem. Eng. 92 (2) (2013) 324–329.
[32] H. Abrahamse, M.R. Hamblin, New photosensitizers for photodynamic therapy, Biochem. J. 473 (4) (2016) 347–364.

[33] K. Hu, X. He, P. Jin, X. Wang, H. Pan, J. Chen, Unravelling the cometition between internal conversion and intersystem crossing in twisted molecule 9-phenylacridine by femtosecond time-resolved spectroscopy, ChemPhotoChem 8 (2024) e202400108.
[34] A.L. Daniel-da-Silva, L. Ferreira, A.M. Gil, T. Trindade, Synthesis and swelling behavior of temperature responsive κ-carrageenan nanogels, J. Colloid Interface Sci. 355 (2) (2011) 512–517.
[35] I.J. Joye, D.J. McClements, Production of nanoparticles by anti-solvent precipitation for use in food systems, Trends Food Sci. Technol. 34 (2) (2013) 109–123.
[36] A. Bahrami, R. Delshadi, S.M. Jafari, L. Williams, Nanoencapsulated nisin: an engineered natural antimicrobial system for the food industry, Trends Food Sci. Technol. 94 (2019) 20–31.
[37] E. Dickinson, Hydrocolloids at interfaces and the influence on the properties of dispersed systems, Food Hydrocoll. 17 (1) (2003) 25–39.
[38] L. Bai, S. Huan, J. Gu, D.J. McClements, Fabrication of oil-in-water nanoemulsions by dual-channel microfluidization using natural emulsifiers: Saponins, phospholipids, proteins, and polysaccharides, Food Hydrocoll. 61 (2016) 703–711.
[39] R. Chanamai, D. McClements, Depletion flocculation of beverage emulsions by gum Arabic and modified starch, J. Food Sci. 66 (3) (2001) 457–463.
[40] D.J. McClements, Food Emulsions: Principles, Practices, and Techniques, CRC press, 2004.
[41] M.S. Orellano, C. Porporatto, J.J. Silber, R.D. Falcone, N.M. Correa, AOT reverse micelles as versatile reaction media for chitosan nanoparticles synthesis, Carbohydr. Polym. 171 (2017) 85–93.
[42] J. Yang, Y. Huang, C. Gao, M. Liu, X. Zhang, Fabrication and evaluation of the novel reduction-sensitive starch nanoparticles for controlled drug release, Colloids Surf. B: Biointerfaces 115 (2014) 368–376.
[43] D. Renard, L. Lavenant-Gourgeon, M.-C. Ralet, C. Sanchez, Acacia senegal gum: continuum of molecular species differing by their protein to sugar ratio, molecular weight, and charges, Biomacromolecules 7 (9) (2006) 2637–2649.
[44] C.F. de Freitas, E. Kimura, A.F. Rubira, E.C. Muniz, Curcumin and silver nanoparticles carried out from polysaccharide-based hydrogels improved the photodynamic properties of curcumin through metal-enhanced singlet oxygen effect, Mater. Sci. Eng. C 112 (2020) 110853.
[45] D.S. No, A. Algburi, P. Huynh, A. Moret, M. Ringard, N. Comito, D. Drider, P. Takhistov, M.L. Chikindas, Antimicrobial efficacy of curcumin nanoparticles against *Listeria monocytogenes* is mediated by surface charge, J. Food Saf. 37 (4) (2017) e12353.
[46] V. Ryu, S. Ruiz-Ramirez, P. Chuesiang, L.A. McLandsborough, D.J. McClements, M. G. Corradini, Use of micellar delivery systems to enhance curcumin's stability and microbial photoinactivation capacity, Foods 10 (8) (2021) 1777.
[47] E. Preis, E. Baghdan, M.R. Agel, T. Anders, M. Pourasghar, M. Schneider, U. Bakowsky, Spray dried curcumin loaded nanoparticles for antimicrobial photodynamic therapy, Eur. J. Pharm. Biopharm. 142 (2019) 531–539.
[48] T. Li, Y. Zhao, K. Matthews, J. Gao, J. Hao, S. Wang, J. Han, Y. Jia, Antibacterial activity against *Staphylococcus aureus* of curcumin-loaded chitosan spray coupled with photodynamic treatment, LWT-Food Science and Technology 134 (2020) 110073.
[49] R. Hariharan, S. Senthilkumar, A. Suganthi, M. Rajarajan, Photodynamic action of curcumin derived polymer modified ZnO nanocomposites, Mater. Res. Bull. 47 (11) (2012) 3090–3099.
[50] P. Comeau, A. Manso, A systematic evaluation of curcumin concentrations and blue light parameters towards antimicrobial photodynamic therapy against cariogenic microorganisms, Pharmaceutics 15 (12) (2023) 2707.
[51] L.S. Sampaio, S.R. de Annunzio, L.M. de Freitas, L.O. Dantas, L. De Boni, M. C. Donatoni, K.T. de Oliveira, C.R. Fontana, Influence of light intensity and irradiation mode on methylene blue, chlorin-e6 and curcumin-mediated photodynamic therapy against *Enterococcus faecalis*, Photodiagn. Photodyn. Ther. 31 (2020) 101925.
[52] D.H. Thompson, O.V. Gerasimov, J.J. Wheeler, Y. Rui, V.C. Anderson, Triggerable plasmalogen liposomes: improvement of system efficiency, Biochimica et Biophysica Acta (BBA)-Biomembranes 1279 (1) (1996) 25–34.
[53] B. Tuccio, R. Lauricella, C. Fréjaville, J.-C. Bouteiller, P. Tordo, Decay of the hydroperoxyl spin adduct of 5-diethoxyphosphoryl-5-methyl-1-pyrroline N-oxide: an EPR kinetic study, J. Chem. Soc. Perkin Trans. 2 (2) (1995) 295–298.
[54] W.Y. Oh, F. Shahidi, Antioxidant activity of resveratrol ester derivatives in food and biological model systems, Food Chem. 261 (2018) 267–273.